ESKİŞEHİR TEKNİK ÜNİVERSİTESİ BİLİM VE TEKNOLOJİ DERGİSİ B- TEORİK BİLİMLER

Eskişehir Technical University Journal of Science and Technology B- Theoretical Sciences

2023, 11(1), pp. 1-12, DOI: 10.20290/estubtdb.1038609

RESEARCH ARTICLE

A THEORETICAL APPROXIMATION FOR LAMINAR FLOW BETWEEN ECCENTRIC CYLINDERS

Egemen OGRETIM [1], * , Hasan CAKMAK [2]

[1] Independent Researcher, Izmir, Turkey
[2] Aegean Dynamics, Izmir, Turkey

ABSTRACT

Taylor-Couette flow between two concentric cylinders has received much attention due to its use in various applications, including biomedical devices, micro electro-mechanical systems, polymer pumping and electric motor cooling. Due to the complex interaction of the viscosity and the involved geometry within the confined space, different flow regimes are dominant under different conditions, affecting the fluid dynamics and heat transfer. In analyzing the mentioned flow, besides the experimental and computational studies, analytical models have been developed with varying levels of complication. In the present study, using the homotopy of both the flow and the domain geometry between the concentric and eccentric cylinders, a practical formula for flow between eccentric cylinders is developed. In doing so, an appropriate transformation function for the geometry is developed and embedded into the velocity equation for the concentric cylinders. The resultant equation is tested against flow simulation results. A validity margin analysis is performed based on the variation of the mass flow rate between the cylinders. It is seen that the proposed model for eccentric cylinders is applicable for all gap distances, unlike the previous models that are restricted to narrow gaps. Finally, a separate formula to quantify the error in the estimates of the present method is also derived, which involves the ratio of the cylinders and the eccentricity.

Keywords: Taylor-Couette flow, Homotopy, Laminar flow, Navier-Stokes, Eccentric cylinders

NOMENCLATURE

r	radial coordinate for the concentric case
r'	radial coordinate for the eccentric case
r^*	dimensionless radial coordinate for the concentric case, r/r_o
r'^*	dimensionless radial coordinate for the eccentric case, r'/r_o
r_i	radius of the inner cylinder
r_o	radius of the outer cylinder
s	distance between the centers
v_θ	tangential velocity for the concentric case
v'_θ	tangential velocity for the eccentric case
v_θ^*	dimensionless tangential velocity, $v_\theta/\omega r_i$
v'^*_θ	dimensionless tangential velocity, $v_\theta/\omega r_i$
$\dot{\forall}$	volume flow rate
x	distance between inner and outer cylinder centers
x^*	dimensionless distance between inner and outer cylinder centers, x/r_o
θ	angular coordinate
ρ	ratio of the radii, r_i/r_o
σ	ratio of distance between the centers and the outer radius, s/r_o
τ	shear stress
ω	angular speed of the inner cylinder

*Corresponding Author: egemenogretim@yahoo.com
Received: 21.12.2021 Published: 28.02.2023

1. INTRODUCTION

Flow between two concentric circles is known as Taylor-Couette flow, and has been studied extensively due to its applications in various fields. These applications include lubrication, heat transfer, bioreactors, magnetohydrodynamics, desalination and pumping. The governing flow in the space between the two cylinders can be steady or unsteady, one-dimensional or multi-dimensional depending on the distance and rotational speeds of the cylinders [1,2]. Therefore, controlling the flow dynamics is of utmost importance to increase the energy efficiency of the involved systems.

Energy efficiency of any given device is important, however, inefficiencies in the performance are not limited to energy. In applications like blood transfusion, Reynolds stresses, wall shear stress and cavitation cause blood damage (hemolysis), hence a loss of the valuable fluid [3,4]. For the suspension cell cultures in a rotating wall vessel, the distribution of the nutrients and the well-being of the growing cells require a careful management of the flow stresses [5].

Cooling of the in-wheel electric motors for the electrically driven cars is another application of flow within narrow cylindrical walls. It is known that the heating of the rotor and stator coils during functioning is a cause for reduced energy efficiency [6]. The flow in the narrow cylindrical volume can be utilized for cooling the motor parts to increase efficiency [7].

A wider range of practical applications can be found if, instead of a geometry that is strictly composed of two concentric cylinders, slight modifications to the Taylor-Couette flow are investigated. Left ventricular assist devices [8], partially filled gaps [9], flow control by means of pressure management in semicircular gaps [10], lubrication between two eccentric cylinders [11,12] and heat transfer control in flow between eccentric cylinders [13] are among such avenues of investigation.

Taylor-Couette flow between eccentric cylinders, which is the focus of the present study, is also relevant to a novel type of pump. This pump can combine two functions, namely heat transfer and flow pumping, in one component. Conventionally, these two functions are performed by the different components within the heat recovery systems. Namely, air flow energized by a fan goes through a heat recovery wheel (Figure 1) for heat transfer purposes. These wheels are large cylinders with narrow channels that are made of a conductive material, such as aluminum. The large cylinder rotates slowly so that the walls of the narrow channels gain and lose heat alternatively upon contact with the relevant fluid, thereby incurring energy savings.

Although viscosity is an adverse effect in case of the conventional heat recovery wheels, hence the need for a fan to push the fluid through the narrow channels, it is the functioning mechanism for the novel pump mentioned above. In this pump, where the eccentric circular structure is present, a cylinder that has closely-placed fin-like walls on it (Figure 2) grabs the fluid within the space between the walls, thanks to the viscosity. Upon rotation of the cylinder, the fluid can gain kinetic energy and then be diverted into a channel where the flow is desired, hence a viscosity-based circulation pump. A careful look can reveal that this device is a modification from the Tesla turbine, which also works on the viscous interaction between the fluid and the solid surfaces.

Due to the symmetry of the geometry, two opposing flows are triggered as a result of the rotation of the cylinder. During the transfer from the inlet side of the cylinder to the outlet side, heat transfer between the fluid and the walls of the cylinder takes place. In order to predict the performance of this device, however, flow between the eccentric circles must be studied.

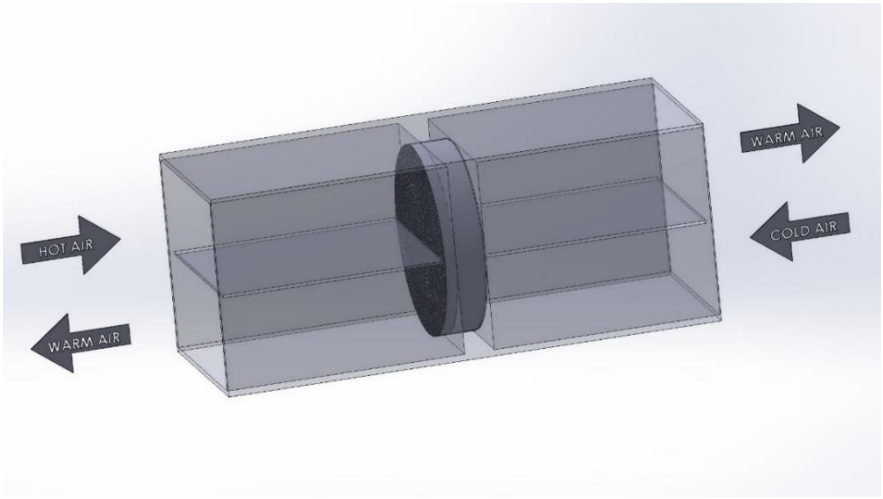

Figure 1. A conventional heat recovery wheel.

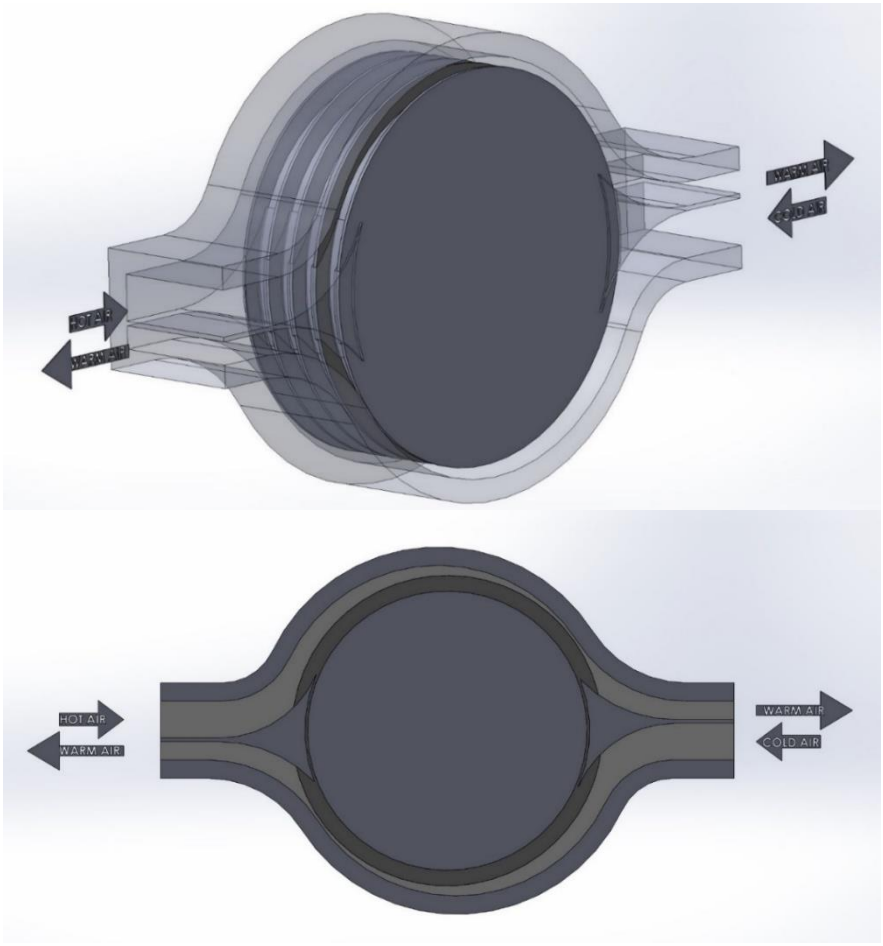

Figure 2. The viscosity-based circulation pump; blown-up perspective view (up), cross-sectional view (bottom).

Another possible application of this viscosity-based pump is in blood transfusion or in artificial hearts. Due to its continuous flow capability, rather than pulsating, there is little to no induced turbulence, hence high efficiency blood transfer [14]. Again, in order to estimate the stress levels that the blood cells are going to be subject to, the Taylor-Couette flow in this eccentric geometry must to be modeled either theoretically or computationally.

Other possible applications of the proposed pump pertains to the field of micropumps. Today, micropumps are used in several major areas, such as drug delivery, dosing systems, space exploration, micro-electronics and fuel cells [15]. This viscosity based recirculation pump can provide continuous and relatively high flow rate. The performance characteristics in such applications, again, demand the knowledge of the contribution of the various parameters to the flow between the eccentric circles.

Present study is aimed at providing a practical formulation for the laminar flow between eccentric circles, where the inner one is rotating at a fixed speed and the outer one is stationary. To arrive at an analytical formula for this flow, steady, incompressible, pseudo one-dimensional flow is assumed. Then, based on the homotopy of the flow domain geometry and the flow, a transformation function is developed between the concentric and the eccentric cases. This transformation is used to modify the velocity equation for the concentric case to the eccentric case.

Following these analytical steps, computational fluid dynamics analyses of the flow between the eccentric cylinders are made. These simulations are performed for various values of the geometrical parameters in the laminar flow regimes. The results from the laminar flow simulations are compared with the analytical solutions and a margin of validity is determined for the approximate formulation derived in this study.

2. DERIVATION OF THE FORMULAE

First step of the theoretical study here involves the geometrical similarity between the concentric and the eccentric cylinders. So, geometric relationships for an eccentric case are derived, first. Following this step, the transformation between the eccentric and the concentric case is formulated to ensure the flow homotopy of the two cases. Finally, the known solution for the concentric cylinders is modified to fit the eccentric case.

2.1. Geometric Relationships

For steady, incompressible flow with no body forces, the tangential flow between two concentric cylinders can be simplified based on the premise that radial and axial velocity components are negligible and that the tangential velocity and the pressure are only functions of the radial coordinate [1]. The resultant momentum equation in the tangential direction is:

$$\frac{d^2 v_\theta}{dr^2} + \frac{d(v_\theta/r)}{dr} = 0 \tag{1}$$

Solving equation1 for an outer cylinder at rest and an inner cylinder at rotation, the resultant axisymmetric solution is given as:

$$v_\theta = \frac{\omega r_i^2}{(r_i^2 - r_o^2)}\left[r - \frac{r_o^2}{r}\right] \tag{2}$$

This formula can readily be used to describe the laminar flow for the concentric case. In the present study, in order to obtain an expression for the velocity distribution between eccentric cylinders, first, a relationship is developed for the alternating distance between the two cylinders (Figure 3). The coordinate center remains as the center of the inner, rotating cylinder (C_i) but the coordinates on the outer cylinder must be redefined due to the shift (s) of the center of the outer cylinder (C_o). Accordingly, the following two relationships can be formulated based on the distances in the horizontal and vertical.

$$r_o \sin\alpha = (r_i + x)\sin\theta \tag{3}$$

$$r_o \cos\alpha = (r_i + x)\cos\theta + s \tag{4}$$

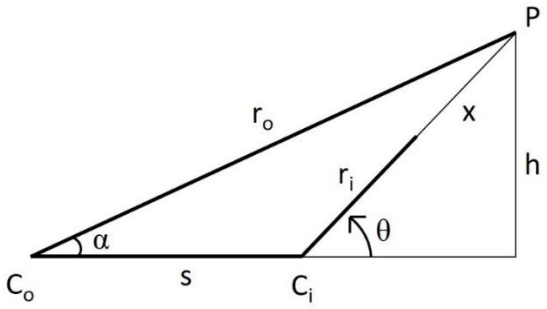

Figure 3. Geometrical representation of the relationship between the design parameters.

Taking the squares of these equations and adding:

$$(r_i + x)^2 + 2s\,(r_i + x)\cos\theta + (s^2 - r_o^2) = 0 \tag{5}$$

In this equation, (r_i+x) can be treated as a single unknown term. Consequently, equation 5 becomes a second order polynomial in terms of (r_i+x). Solving this polynomial and rearranging for x:

$$x = \sqrt{r_o^2 - s^2\sin^2\theta} - s\cos\theta - r_i \tag{6}$$

This expression gives the width of the gap at the angular position between the eccentric cylinders.

2.2. Transformation Function

Before starting the details of the transformation function, it is necessary to talk about the concept of homotopy. In the topology branch of mathematics, if two geometries or functions can be transformed to each other only by squeezing and stretching of their parts, then they are called homotopic (Figure 4).

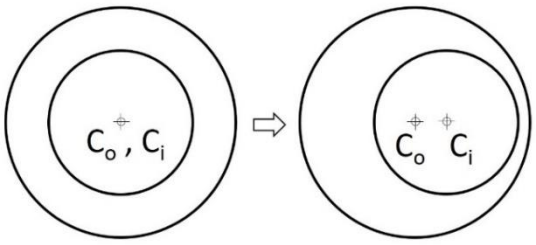

Figure 4. Homotopic transformation of the concentric and the eccentric cases.

When the concentric and the eccentric cylinders are considered, it is obvious that one can be deformed into the other, without needing a cut or gluing. However, if one increases the amount of eccentricity by bringing the inner cylinder to an almost tangent state with the outer one, then, although the homotopy of the initial and final geometries is satisfied, resultant flow fields are not going to be similar. Whereas the initial case of concentric cylinders is going to have streamlines in the form of concentric circles, the eccentric case is going to develop recirculation zones with increasing eccentricity [16]. So, there is a limit to the eccentricity in terms of conserving the structure of the flow fields. This second property about the flow structure is linked to the Hairy Ball Theorem of topology. Expressed in terms of the flow field of concern here, the number of centers of rotation must be conserved through the homotopic transformation of the geometries.

Aside from these two conditions, there are two more physical properties that need to be conserved. First is the no slip condition that states that the velocity field must match the velocity of the solid surfaces at the points of contact. No slip condition can easily be expressed for the concentric case, since the radial coordinate of both the inner and the outer cylinder is constant. For the eccentric case, however, at every angular coordinate, although the inner periphery has a constant radial position, the outer periphery is changing. This change of width has been formulated above, however, the same change must also be embedded into the final velocity distribution for the eccentric case.

Second condition for the validity of the transformed velocity distribution is the conservation of mass flow rate. This condition can be satisfied in two ways. First, the individual streamlines are modified in such a way to ensure the constancy of the mass flow rate over the gap at a given angular position. The second way to satisfy the constancy of the mass flow rate is by ensuring the same mass flow rate in each streamline. This last method, which is the one assumed for the present study, can be expressed mathematically as follows:

$$v_\theta \, dr = \, v'_\theta \, dr' \tag{7}$$

In consideration for the first stipulation about the no slip condition, the expression for conservation of mass can slightly be modified as follows:

$$v'_\theta \, = v_\theta \frac{dr}{dr'} \tag{8}$$

Thus, at the inner periphery and the outer periphery, the derivative term in equation 8 must have a value of 1 so that the no slip condition can be satisfied with the same values as the concentric case. Therefore, a transformation function is needed between the radial coordinates of the concentric and the eccentric cases, which has the specified derivative value at the periphery.

The below transformation function has been discovered in the present study, satisfying all of these conditions.

$$r = r' - x \sin^2\left[\frac{(r'-r_i)}{x}\frac{\pi}{2}\right] + (r_o - r_i)\cos^2\left[\frac{(r'-r_i-x)}{x}\frac{\pi}{2}\right] \tag{9}$$

Taking the derivative of r with respect to r':

$$\frac{dr}{dr'} = 1 - \frac{\pi}{2}\sin\left[\frac{(r'-r_i)}{x}\pi\right] - \frac{\pi\,(r_o-r_i)}{2x}\sin\left[\frac{(r'-r_i-x)}{x}\pi\right] \tag{10}$$

Non-dimensionalizing equations 9 and 10 by r_o, the following are obtained:

$$r^* = r'^* - x^* \sin^2\left[\frac{(r'^*-\rho)}{x^*}\frac{\pi}{2}\right] + (1-\rho)\cos^2\left[\frac{(r'^*-\rho-x^*)}{x^*}\frac{\pi}{2}\right] \tag{11}$$

$$\frac{dr^*}{dr'^*} = 1 - \frac{\pi}{2}\sin\left[\frac{(r'^*-\rho)}{x^*}\pi\right] - \frac{\pi\,(1-\rho)}{2x^*}\sin\left[\frac{(r'^*-\rho-x^*)}{x^*}\pi\right] \tag{12}$$

where $r^* = r/r_o$, $r'^* = r'/r_o$, $\rho = r_i/r_o$, $\sigma = s/r_o$, $x^* = x/r_o$.

In order to show what this transformation means in terms of the radial coordinates and the velocity distribution, the equations 11 and 12 are plotted for ρ=0.6 and σ =0.05 in Figure 5. The angles indicated in the graphs are in degrees.

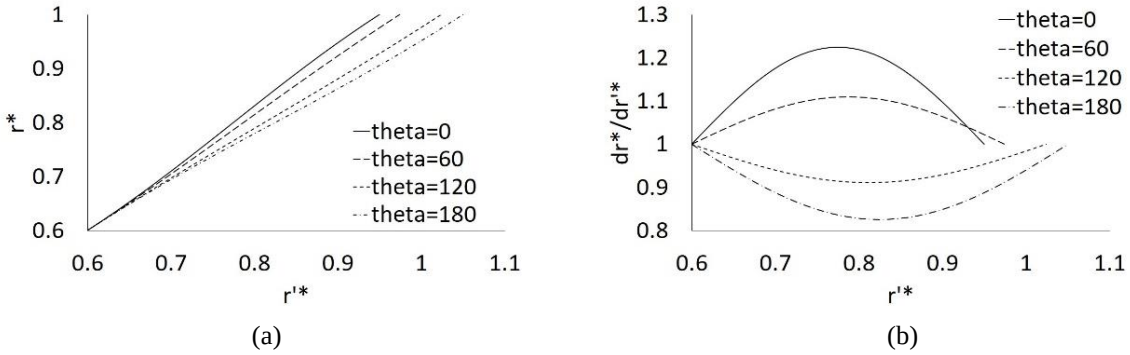

(a) (b)

Figure 5. Variation of r* (a) and its derivative (b) with respect to r'*.

For the 0 degree, as seen in Figure 4, the radius is decreased, whereas for the 180 degree, it is increased, both of which are reflected in the smaller and larger values of r'*, respectively. Still, for all angles, the derivative of r* with respect to r'* is equal to unity at the solid walls in order to satisfy the no slip condition as described through the equation 8. In between, however, for the contracted spaces, the velocity is increased, as indicated by the growing values of the derivative, whereas for the expanded spaces, the velocity is decreased by virtue of the derivative values less than unity.

An implied assumption in equation 8 is that the velocity is normal to the radial direction. This is the case for the concentric setting. However, due to the alternating width of the space between the cylinders in the eccentric case, such orthogonality is not always the case. Still, the formulation in this study assumes it, which means an inconsistency between this theory and the physics for the locations where the orthogonality is violated. This violation is especially present near the outer wall, where there is zero velocity due to the no slip condition. Therefore, even if the theory has deficiency in explaining the locations near the outer wall, it is not to a large degree due to the negligible magnitude of the velocity there.

2.3 Validity Margin Analysis

The velocity transformation chosen in this study necessitates that the volume flow rate along every streamline stay constant during the transformation from the concentric case to the eccentric case. This also translates to the fact that the overall volume flow rate within the flow must remain constant. However, it is obvious that as the eccentricity increases, the gap between the cylinders eventually closes on one side, which points at a gradually decreasing volume flow rate with eccentricity (Figure 6).

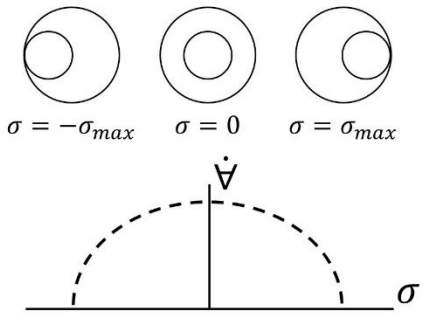

Figure 6. Qualitative form of variation of volume flow rate with eccentricity.

So, in order to approximate the change in the overall volume flow rate, a mathematical expression is needed, which can also be useful for determining a margin of validity for the transformation function proposed in this article.

Looking at Figure 6, there are three known boundary conditions for the function that is describing the variation of overall volume flow rate between the cylinders:

1. when eccentricity is zero, volume flow rate is equal to that of the concentric case,

$$\sigma = 0 \qquad \dot{\forall} = \dot{\forall}_c$$

2. when eccentricity is equal to the distance between the cylinders, volume flow rate is zero,

$$\sigma = 1-\rho \qquad \dot{\forall} = 0$$

3. when the eccentricity is zero, the derivative of volume flow rate with respect to eccentricity is zero; this condition stems from the fact that the physics of the problem is symmetric in terms of the variation of volume flow rate with eccentricity (Figure 6),

$$\sigma = 0 \qquad \frac{d\dot{\forall}}{d\sigma} = 0$$

Considering this limited amount of information for the variation with eccentricity, a simple, two-term Fourier expansion can be employed to emulate the behavior of the volume flow rate.

$$\dot{\forall} = A\cos(\lambda\sigma) + B\sin(\lambda\sigma) \tag{13}$$

The third boundary condition mentioned above requires that B=0. The second condition brings to the following result:

$$A\cos[\lambda(1-\rho)] = 0 \tag{14}$$

Since A cannot be zero, then the cosine term must be equal to zero.

$$\lambda(1-\rho) = \frac{\pi}{2}(2n-1) \tag{15}$$

Choosing n=1 for a simple approximation,

$$\lambda = \frac{\pi}{2(1-\rho)} \tag{16}$$

Then, the volume flow rate expression becomes:

$$\dot{\forall} = A\cos\left[\frac{\pi\sigma}{2(1-\rho)}\right] \tag{17}$$

The remaining condition, that is the first condition for the concentric case gives the value of *A*.

$$A = \dot{\forall}_c \tag{18}$$

The value of *A*, i.e. the volume flow rate for the concentric case, can be obtained by integrating the equation 2 over the radial coordinate from inner cylinder to the outer cylinder, which gives:

$$A = \omega\, r_i^2 \left[\frac{\ln \rho}{(1-\rho^2)} - \frac{1}{2}\right] \tag{19}$$

The final expression for the overall volume flow rate becomes:

$$\dot{\forall} = \omega\, r_i^2 \left[\frac{\ln \rho}{(1-\rho^2)} - \frac{1}{2}\right] \cos\left[\frac{\pi\sigma}{2(1-\rho)}\right] \tag{20}$$

Here, the terms other than the cosine are only about the value for the concentric case and it is only the cosine term that determines the fraction of that amount in case of eccentricity. So, a value of 1 for the cosine term refers to the concentric case, and values less than 1 to the eccentric cases. However, the velocity profile described through equations 8 and 12 is derived in a way to conserve the volume flow rate during the transformation. So, as the eccentricity increases, the new velocity profile is going to accrue error. In order to quantize this error, one can insert values of ρ into the cosine term in equation 20, and produce an equation for the limit of σ. For example, if an error of 5% in volume flow rate is acceptable, then:

$$\cos\left[\frac{\pi\sigma_{max}}{2(1-\rho)}\right] = 0.95 \tag{21}$$

That is, for a given value of ρ and a maximum acceptable error of 5% in volume flow rate, one can use σ values up to the σ_{max} that comes out of the above expression. Approximately, this is equal to:

$$\sigma_{max,5\%\, error} = 0.2022\,(1-\rho) \tag{22}$$

The same procedure can be performed for different values of acceptable error in the volume flow rate and the corresponding equations for the maximum acceptable eccentricity can be obtained and plotted.

3. RESULTS AND DISCUSSION

The variation of maximum acceptable eccentricity with the ratio of the radii of the cylinders is shown in Figure 7. Naturally, as the error margin is released, higher levels of eccentricity can be handled by the formulation given in the present study. However, for the same error margin, increase of the radius of inner circle, hence higher values of ρ, leads to smaller values of for the upper limit of eccentricity. This is due to the fact that the flow is more easily blocked by the movement of the inner cylinder for high values of ρ compared to the lower ones. So, error in the mass flow rate rapidly increases with eccentricity, leading to the mentioned result. A noteworthy advantage that becomes obvious through this error analysis is that the model presented in this study can be used even for large gaps between the cylinders, unlike the most previous studies that address exclusively narrow gaps. Also, the range of velocity does not have to be in the Stokes flow range, but can be higher, as long as the flow is laminar and without recirculation zones.

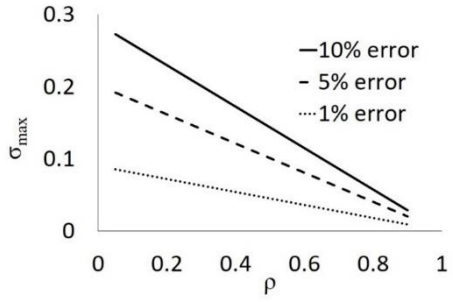

Figure 7. Maximum acceptable eccentricity for different values of error.

When equations 2, 8 and 12 are used and the results are non-dimensionalized for the flow between eccentric cylinders, detailed tangential velocity distribution can be obtained at different angles. Here, as an example, the results for ρ=0.1 is presented σ=0.1 (Figure 8). Since this is a steady flow and since the flow is symmetric in the upper and lower halves, only the velocity profiles at angles between 0, 90 and 180 degrees are plotted. In Figure 8, the curve for 0 degrees represents the narrowest passage between the cylinders, whereas the curve for 180 degrees shows the largest passage. By virtue of having the same mass flow rate, hence equal areas under the curves, a more rapid drop in velocity is observed in the 180 degree case in the vicinity of the inner cylinder. However, the reach of the momentum due to the rotation of the inner cylinder is farther at 180 degrees, hence the extra mass flow to make up for the missing flow rate towards the center.

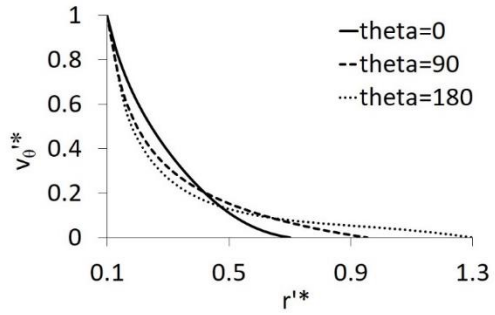

Figure 8. Variation of tangential velocity with radial position for ρ = 0.1 and σ = 0.3.

As a verification, the same case is simulated computationally using the Solidworks commercial software. The resultant tangential velocity distribution is shown in Figure 9. Comparing Figure 8 and Figure 9, it is seen that there is a general agreement between the analytical results and the simulated ones. The difference between the two is especially observed within the vicinity of the inner cylinder. Nevertheless, the effects of conservation of mass at different angular positions, i.e. the constancy of area under the curves, is observed in the simulated results, too.

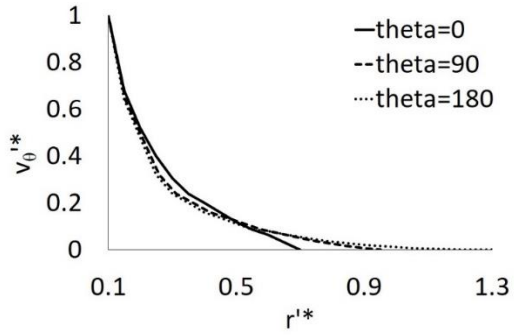

Figure 9. Simulated tangential velocity with radial position for ρ = 0.1 and σ = 0.3.

4. CONCLUSION

In this study, a transformation function is developed to define the tangential velocity distribution for flow between two eccentric cylinders. The function takes the velocity distribution of the concentric case for the same cylinder radii and transforms it to the eccentric case using a conformal mapping between the two shapes and the conservation of mass. The resultant formulation is applicable for the laminar flow without recirculation zones. Unlike most previous studies, there is no limitation to the gap width in this formulation. In order to quantify and limit the error of the proposed function, another formula is

derived that tells the maximum acceptable eccentricity for a given ratio of cylinder radii. The formulation produced in this study can help with the design and improvement of the devices involving eccentric cylinders, such as can be found in lubrication, heat transfer or blood transfusion.

ACKNOWLEDGEMENTS

The authors would like to thank Ses3000, Ltd. in Izmir, TURKEY, for their support of this study.

CONFLICT OF INTEREST

The authors stated that there are no conflicts of interest regarding the publication of this article.

REFERENCES

[1] Fénot M, Bertin Y, Dorignac E, Lalizel G. A review of heat transfer between concentric rotating cylinders with or without axial flow. Int J Therm Sci, 2011; 50: 1138-1155.

[2] Wen J, Zhang WY, Ren LZ, Bao LY, Dini D, Xi HD, Hu HB. Controlling the number of vortices and torque in Taylor-Couette flow. J Fluid Mech 2020; 901: A30.

[3] Deutsch S, Tarbell JM, Manning KB, Rosenberg G, Fontaine AA. Experimental fluid mechanics of pulsatile artificial blood pumps. Annu Rev Fluid Mech, 2006; 38: 65-86.

[4] Goubergrits L, Osman J, Mevert R, Kertzscher U, Pöthkow K, Hege HC. Turbulence in blood damage modeling. Int J Artif Organs, 2016; 39(4): 160-165.

[5] Hammond TG, Hammond JM. Optimized suspension culture: The rotating-wall vessel. Am J Physiol-Renal, 2001; 281: F12-F25.

[6] Lim DH, Lee MY, Lee HS, Kim SC. Performance evaluation of an in-wheel motor cooling system in an electric vehicle/hybrid electric vehicle. Energies, 2014; 7: 961-971.

[7] Li H. Cooling of a permanent magnet electric motor with a centrifugal impeller. Int J Heat Mass Tran, 2010; 53: 797-810.

[8] Abe Y, Ishii K, Isoyama T, Saito I, Inoue Y, Ono T, Nakagawa H, Nakano E, Fukazawa K, Ishihara K, Fukunaga K, Ono M, Imachi K. The helical flow pump with a hydrodynamics levitation impeller. J Artif Organs, 2012; 15: 331-340.

[9] Mukunda PG, Shailesh RA, Kiran AS, Shrikantha SR. Experimental studies of flow patterns of different fluids in a partially filled rotating cylinder. J Appl Fluid Mech, 2009; 2(1): 39-43.

[10] Lebiga VA, Pak AY, Zinoyev VN, Mironov DS, Medvedev AE. Simulation of Couette flow in semicircular channel. AIP Conf Proceed, 2019; 030017.

[11] Diprima RC, Stuart JT. Flow between Eccentric Rotating Cylinders. J Lubric Tech, 1971; 72-Lub-J.

[12] Saatdjian E, Midoux N. Flow of a Newtonian fluid between eccentric rotating cylinders. Int J Numer Meth Heat Fluid Fl, 1992; 2: 261-270.

[13] Teleszewski TJ. Effect of viscous dissipation in Stokes flow between rotating cylinders using BEM. Int J Numer Meth Heat Fluid Fl, 2020; 30(4): 2121-2136.

[14] Faghih MM, Sharp MK. Evaluation of energy dissipation rate as a predictor of mechanical blood damage. Artif Organs, 2018; 43: 666-676.

[15] Mohith S, Karanth PN, Kulkarni SM. Recent trends in mechanical micropumps and their applications: A review. Mechatronics, 2019; 60: 34-55.

[16] Dai RX, Dong Q, Szeri AZ. Flow between Eccentric Rotating Cylinders: Bifurcation and Stability. Int J Eng Sci, 1992; 30(10): 1323-1340.